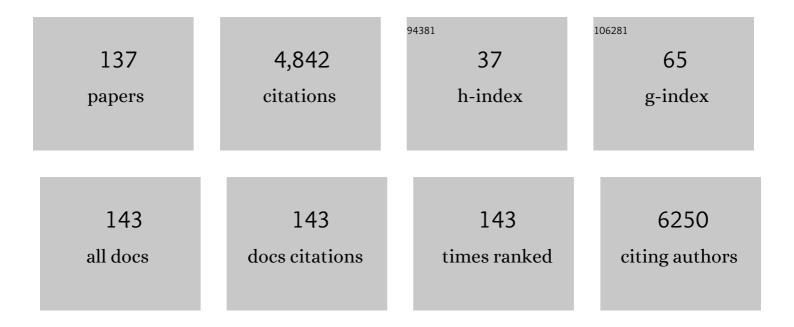
List of Publications by Year in descending order

Source: https://exaly.com/author-pdf/2441603/publications.pdf Version: 2024-02-01



#	Article	IF	CITATIONS
1	Selective Growth of Well-Aligned Semiconducting Single-Walled Carbon Nanotubes. Nano Letters, 2009, 9, 800-805.	4.5	426
2	Real Space Mapping of Li-Ion Transport in Amorphous Si Anodes with Nanometer Resolution. Nano Letters, 2010, 10, 3420-3425.	4.5	232
3	Differentiating Ferroelectric and Nonferroelectric Electromechanical Effects with Scanning Probe Microscopy. ACS Nano, 2015, 9, 6484-6492.	7.3	231
4	Mechanism of NO2 detection in carbon nanotube field effect transistor chemical sensors. Applied Physics Letters, 2006, 88, 123112.	1.5	158
5	Symmetry Relationship and Strain-Induced Transitions between Insulating M1 and M2 and Metallic R phases of Vanadium Dioxide. Nano Letters, 2010, 10, 4409-4416.	4.5	149
6	Doping-Based Stabilization of the M2 Phase in Free-Standing VO ₂ Nanostructures at Room Temperature. Nano Letters, 2012, 12, 6198-6205.	4.5	145
7	Nanoscale Ferroelectricity in Crystalline γâ€Glycine. Advanced Functional Materials, 2012, 22, 2996-3003.	7.8	119
8	Evidence for power-law frequency dependence of intrinsic dielectric response in theCaCu3Ti4O12. Physical Review B, 2004, 70, .	1.1	110
9	The Role of Electrochemical Phenomena in Scanning Probe Microscopy of Ferroelectric Thin Films. ACS Nano, 2011, 5, 5683-5691.	7.3	109
10	Interplay between Ferroelastic and Metalâ^'Insulator Phase Transitions in Strained Quasi-Two-Dimensional VO ₂ Nanoplatelets. Nano Letters, 2010, 10, 2003-2011.	4.5	101
11	Interplay of Octahedral Tilts and Polar Order in BiFeO ₃ Films. Advanced Materials, 2013, 25, 2497-2504.	11.1	101
12	Tracking ion intercalation into layered Ti ₃ C ₂ MXene films across length scales. Energy and Environmental Science, 2020, 13, 2549-2558.	15.6	100
13	Probing charge screening dynamics and electrochemical processes at the solid–liquid interface with electrochemical force microscopy. Nature Communications, 2014, 5, 3871.	5.8	97
14	Quantification of surface displacements and electromechanical phenomena via dynamic atomic force microscopy. Nanotechnology, 2016, 27, 425707.	1.3	92
15	Microwave a.c. conductivity of domain walls in ferroelectric thin films. Nature Communications, 2016, 7, 11630.	5.8	81
16	Big data and deep data in scanning and electron microscopies: deriving functionality from multidimensional data sets. Advanced Structural and Chemical Imaging, 2015, 1, 6.	4.0	74
17	Li-ion dynamics and reactivity on the nanoscale. Materials Today, 2011, 14, 548-558.	8.3	73
18	Atomicâ€Level Sculpting of Crystalline Oxides: Toward Bulk Nanofabrication with Single Atomic Plane Precision. Small, 2015, 11, 5895-5900.	5.2	73

#	Article	IF	CITATIONS
19	Dimensionality Controlled Octahedral Symmetry-Mismatch and Functionalities in Epitaxial LaCoO ₃ /SrTiO ₃ Heterostructures. Nano Letters, 2015, 15, 4677-4684.	4.5	71
20	Nonlinear Phenomena in Multiferroic Nanocapacitors: Joule Heating and Electromechanical Effects. ACS Nano, 2011, 5, 9104-9112.	7.3	69
21	Mesoscopic Metalâ~'Insulator Transition at Ferroelastic Domain Walls in VO ₂ . ACS Nano, 2010, 4, 4412-4419.	7.3	68
22	Open loop Kelvin probe force microscopy with single and multi-frequency excitation. Nanotechnology, 2013, 24, 475702.	1.3	63
23	Magnetically Induced Field Effect in Carbon Nanotube Devices. Nano Letters, 2007, 7, 960-964.	4.5	62
24	Direct Mapping of Ionic Transport in a Si Anode on the Nanoscale: Time Domain Electrochemical Strain Spectroscopy Study. ACS Nano, 2011, 5, 9682-9695.	7.3	61
25	Current and surface charge modified hysteresis loops in ferroelectric thin films. Journal of Applied Physics, 2015, 118, .	1.1	60
26	Cross-beam pulsed laser deposition: General characteristic. Review of Scientific Instruments, 2001, 72, 2665-2672.	0.6	53
27	Electromechanical Actuation and Current-Induced Metastable States in Suspended Single-Crystalline VO ₂ Nanoplatelets. Nano Letters, 2011, 11, 3065-3073.	4.5	53
28	Near-field microwave scanning probe imaging of conductivity inhomogeneities in CVD graphene. Nanotechnology, 2012, 23, 385706.	1.3	51
29	Dual harmonic Kelvin probe force microscopy at the graphene–liquid interface. Applied Physics Letters, 2014, 104, .	1.5	50
30	Seeing through Walls at the Nanoscale: Microwave Microscopy of Enclosed Objects and Processes in Liquids. ACS Nano, 2016, 10, 3562-3570.	7.3	47
31	Giant negative electrostriction and dielectric tunability in a van der Waals layered ferroelectric. Physical Review Materials, 2019, 3, .	0.9	47
32	Broadband dielectric microwave microscopy on micron length scales. Review of Scientific Instruments, 2007, 78, 044701.	0.6	44
33	Electrostrictive and electrostatic responses in contact mode voltage modulated scanning probe microscopies. Applied Physics Letters, 2014, 104, 232901.	1.5	44
34	Origins of <mml:math <br="" xmlns:mml="http://www.w3.org/1998/Math/MathML">display="inline"><mml:mrow><mml:mn>1</mml:mn><mml:mo>â^•</mml:mo><mml:mi>f</mml:mi>in individual semiconducting carbon nanotube field-effect transistors. Physical Review B, 2008, 77, .</mml:mrow></mml:math>	w> ₄/ıı nml:ı	nat a s noise
35	Giant elastic tunability in strained BiFeO3 near an electrically induced phase transition. Nature Communications, 2015, 6, 8985.	5.8	43
36	Quantification of in-contact probe-sample electrostatic forces with dynamic atomic force microscopy. Nanotechnology, 2017, 28, 065704.	1.3	43

#	Article	IF	CITATIONS
37	Free tanding Ferroelectric Nanotubes Processed via Softâ€Template Infiltration. Advanced Materials, 2012, 24, 1160-1165.	11.1	38
38	Kelvin probe force microscopy in liquid using electrochemical force microscopy. Beilstein Journal of Nanotechnology, 2015, 6, 201-214.	1.5	38
39	Microwave Impedance Spectroscopy of Dense Carbon Nanotube Bundles. Nano Letters, 2008, 8, 152-156.	4.5	37
40	Probing Local Bias-Induced Transitions Using Photothermal Excitation Contact Resonance Atomic Force Microscopy and Voltage Spectroscopy. ACS Nano, 2015, 9, 1848-1857.	7.3	37
41	Big data in reciprocal space: Sliding fast Fourier transforms for determining periodicity. Applied Physics Letters, 2015, 106, .	1.5	35
42	In situ X-ray microdiffraction studies inside individual VO2 microcrystals. Acta Materialia, 2013, 61, 2751-2762.	3.8	34
43	Big-Data Reflection High Energy Electron Diffraction Analysis for Understanding Epitaxial Film Growth Processes. ACS Nano, 2014, 8, 10899-10908.	7.3	34
44	Mapping internal structure of coal by confocal micro-Raman spectroscopy and scanning microwave microscopy. Fuel, 2014, 126, 32-37.	3.4	34
45	A photolithographic process for fabrication of devices with isolated single-walled carbon nanotubes. Nanotechnology, 2004, 15, 1475-1478.	1.3	33
46	High-resolution dielectric characterization of minerals: A step towards understanding the basic interactions between microwaves and rocks. International Journal of Mineral Processing, 2016, 151, 8-21.	2.6	31
47	Piezoresponse amplitude and phase quantified for electromechanical characterization. Journal of Applied Physics, 2020, 128, .	1.1	31
48	Nanometer-scale mapping of irreversible electrochemical nucleation processes on solid Li-ion electrolytes. Scientific Reports, 2013, 3, 1621.	1.6	29
49	Nonlinear space charge dynamics in mixed ionic-electronic conductors: Resistive switching and ferroelectric-like hysteresis of electromechanical response. Journal of Applied Physics, 2014, 116, 066808.	1.1	29
50	Defect thermodynamics and kinetics in thin strained ferroelectric films: The interplay of possible mechanisms. Physical Review B, 2014, 89, .	1.1	28
51	Acoustic Detection of Phase Transitions at the Nanoscale. Advanced Functional Materials, 2016, 26, 478-486.	7.8	28
52	Features of the film-growth conditions by cross-beam pulsed-laser deposition. Applied Physics A: Materials Science and Processing, 1999, 69, 353-358.	1.1	27
53	Humidity Effect on Nanoscale Electrochemistry in Solid Silver Ion Conductors and the Dual Nature of Its Locality. Nano Letters, 2015, 15, 1062-1069.	4.5	27
54	Surface Control of Epitaxial Manganite Films <i>via</i> Oxygen Pressure. ACS Nano, 2015, 9, 4316-4327.	7.3	27

#	Article	lF	CITATIONS
55	Near-field microwave microscope with improved sensitivity and spatial resolution. Review of Scientific Instruments, 2003, 74, 3167-3170.	0.6	26
56	Spatially Resolved Mapping of Oxygen Reduction/Evolution Reaction on Solid-Oxide Fuel Cell Cathodes with Sub-10 nm Resolution. ACS Nano, 2013, 7, 3808-3814.	7.3	25
57	Nanoscale Mapping of the Double Layer Potential at the Graphene–Electrolyte Interface. Nano Letters, 2020, 20, 1336-1344.	4.5	25
58	Scanning Nearâ€Field Microwave Microscopy of VO ₂ and Chemical Vapor Deposition Graphene. Advanced Functional Materials, 2013, 23, 2635-2645.	7.8	24
59	Learning from Imperfections: Predicting Structure and Thermodynamics from Atomic Imaging of Fluctuations. ACS Nano, 2019, 13, 718-727.	7.3	24
60	Nanoscale Lubrication of Ionic Surfaces Controlled via a Strong Electric Field. Scientific Reports, 2015, 5, 8049.	1.6	23
61	Structural investigations of laser-deposited Fe/Al multilayers. Applied Physics A: Materials Science and Processing, 1999, 68, 497-503.	1.1	22
62	Self-consistent modeling of electrochemical strain microscopy of solid electrolytes. Nanotechnology, 2014, 25, 445701.	1.3	22
63	An atomic force microscopy mode for nondestructive electromechanical studies and its application to diphenylalanine peptide nanotubes. Ultramicroscopy, 2018, 185, 49-54.	0.8	22
64	Zero-bias anomaly and possible superconductivity in single-walled carbon nanotubes. Physical Review B, 2006, 74, .	1.1	21
65	A self-forming nanocomposite concept for ZnO-based thermoelectrics. Journal of Materials Chemistry A, 2018, 6, 13386-13396.	5.2	21
66	X-ray investigation of metastable crystalline phases in co-deposited Fe–Cr alloy nanometer films. Journal of Alloys and Compounds, 2002, 334, 159-166.	2.8	19
67	Toward Quantitative Electrochemical Measurements on the Nanoscale by Scanning Probe Microscopy: Environmental and Current Spreading Effects. ACS Nano, 2013, 7, 8175-8182.	7.3	19
68	Oxygen Control of Atomic Structure and Physical Properties of SrRuO3 Surfaces. ACS Nano, 2013, 7, 4403-4413.	7.3	19
69	Breaking the limits of structural and mechanical imaging of the heterogeneous structure of coal macerals. Nanotechnology, 2014, 25, 435402.	1.3	19
70	Polarization Control via He-Ion Beam Induced Nanofabrication in Layered Ferroelectric Semiconductors. ACS Applied Materials & Interfaces, 2016, 8, 7349-7355.	4.0	19
71	Electromechanical properties of electrostrictive CeO2:Gd membranes: Effects of frequency and temperature. Applied Physics Letters, 2017, 110, .	1.5	19
72	Comparative study of interfaces of Fe–Al multilayers prepared by direct and crossed-beam pulsed laser deposition. Thin Solid Films, 2001, 391, 47-56.	0.8	18

#	Article	IF	CITATIONS
73	Structural and magnetic phase transformation in metastable Fe–Cr alloys induced by ion irradiation. Journal of Applied Physics, 2002, 92, 572-577.	1.1	18
74	Ion transport and softening in a polymerized ionic liquid. Nanoscale, 2015, 7, 947-955.	2.8	18
75	Atomic-scale electrochemistry on the surface of a manganite by scanning tunneling microscopy. Applied Physics Letters, 2015, 106, .	1.5	17
76	Selective patterning of out-of-plane piezoelectricity in MoTe2 via focused ion beam. Nano Energy, 2021, 79, 105451.	8.2	17
77	Fabrication of magnetic nanostructures by direct laser interference lithography on supersaturated metal mixtures. Applied Physics A: Materials Science and Processing, 1999, 69, S819-S822.	1.1	15
78	Carbon nanotubes as nanoscale probes of the superconducting proximity effect in Pd-Nb junctions. Physical Review B, 2009, 80, .	1.1	15
79	The search for superconductivity at van Hove singularities in carbon nanotubes. Superconductor Science and Technology, 2012, 25, 124005.	1.8	15
80	Statics and dynamics of ferroelectric domains in molecular multiaxial ferroelectric (Me ₃ NOH) ₂ [KCo(CN) ₆]. Journal of Materials Chemistry C, 2021, 9, 10741-10748.	2.7	15
81	Magneto-optical properties of Co–Pd alloy films with perpendicular magnetic anisotropy. Journal of Magnetism and Magnetic Materials, 1998, 185, 258-264.	1.0	14
82	Probing Local Electromechanical Effects in Highly Conductive Electrolytes. ACS Nano, 2012, 6, 10139-10146.	7.3	14
83	In Aqua Electrochemistry Probed by XPEEM: Experimental Setup, Examples, and Challenges. Topics in Catalysis, 2018, 61, 2195-2206.	1.3	14
84	Co–Pd alloy films for magneto-optical recording. Journal of Magnetism and Magnetic Materials, 1999, 193, 174-176.	1.0	13
85	Formation of unusual intermetallic phases by vacuum PLD. Applied Surface Science, 2002, 197-198, 475-480.	3.1	13
86	Controlled Nanopatterning of a Polymerized Ionic Liquid in a Strong Electric Field. Advanced Functional Materials, 2015, 25, 805-811.	7.8	13
87	Growth Mode Transition in Complex Oxide Heteroepitaxy: Atomically Resolved Studies. Crystal Growth and Design, 2016, 16, 2708-2716.	1.4	13
88	Near-field microwave microscopy of high- <i>κ</i> oxides grown on graphene with an organic seeding layer. Applied Physics Letters, 2013, 103, .	1.5	12
89	Thermally stimulated crystalline phase transformations in metastable Fe–Cr alloy films prepared by pulsed laser deposition. Journal of Alloys and Compounds, 2002, 347, 171-177.	2.8	11
90	Spatially-resolved mapping of history-dependent coupled electrochemical and electronical behaviors of electroresistive NiO. Scientific Reports, 2014, 4, 6725.	1.6	11

#	Article	IF	CITATIONS
91	Correlative Confocal Raman and Scanning Probe Microscopy in the Ionically Active Particles of LiMn2O4 Cathodes. Materials, 2019, 12, 1416.	1.3	11
92	Thermally stimulated solid state reactions in Fe–Al multilayers prepared by pulsed laser deposition. Journal of Alloys and Compounds, 2001, 320, 114-125.	2.8	10
93	Spatio-energetical characteristics of laser plasma in cross-beam pulsed laser deposition. Applied Surface Science, 1999, 138-139, 12-16.	3.1	8
94	<title>Cross-beam pulsed laser deposition of ultrathin multilayer metal films</title> . , 1999, , .		8
95	Synthesis and frequency-dependent dielectric properties of epitaxial La _{1.875} Sr _{0.125} NiO ₄ thin films. Journal Physics D: Applied Physics, 2012, 45, 305302.	1.3	8
96	Effects of lateral and substrate constraint on the piezoresponse of ferroelectric nanostructures. Applied Physics Letters, 2012, 101, 112901.	1.5	8
97	The Ehrlich–Schwoebel barrier on an oxide surface: a combined Monte-Carlo and <i>in situ</i> scanning tunneling microscopy approach. Nanotechnology, 2015, 26, 455705.	1.3	8
98	Local coexistence of VO2 phases revealed by deep data analysis. Scientific Reports, 2016, 6, 29216.	1.6	8
99	Mn-Doped BaTiO3Ceramics: Thermal and Electrical Properties for Multicaloric Applications. Materials, 2019, 12, 3592.	1.3	8
100	Quantitative Nanometer cale Mapping of Dielectric Tunability. Advanced Materials Interfaces, 2015, 2, 1500088.	1.9	7
101	xmlns:mml="http://www.w3.org/1998/Math/MathML"> <mml:mrow><mml:mi mathvariant="normal">L<mml:msub><mml:mi mathvariant="normal">a<mml:mrow><mml:mn>1</mml:mn><mml:mo>â^`</mml:mo><mml:mi>xmathvariant="normal">C</mml:mi><mml:msub><mml:mi< td=""><td>ml:mi><td>1m1:mrow><!--</td--></td></td></mml:mi<></mml:msub></mml:mrow></mml:mi </mml:msub></mml:mi </mml:mrow>	ml:mi> <td>1m1:mrow><!--</td--></td>	1m 1: mrow> </td
102	mathvariant="normal">a <mml:mi>Mn</mml:mi> <mml:msub><mr Structure of Laser-Deposited Fe/Al Multilayers. Materials Science Forum, 1998, 287-288, 455-458.</mr </mml:msub>	nl:mi 0.3	6
103	Effect of silver doping on the surface of La5/8Ca3/8MnO3 epitaxial films. Applied Physics Letters, 2014, 105, .	1.5	6
104	In-situ near-field probe microscopy of plasma processing. Applied Physics Letters, 2018, 113, 263101.	1.5	6
105	Local electromechanical response in doped ceria: Rigorous analysis of the phase and amplitude. IEEE Transactions on Dielectrics and Electrical Insulation, 2020, 27, 1478-1485.	1.8	6
106	Near-Field Microwave Microscopy: Subsurface Imaging for In Situ Characterization. IEEE Microwave Magazine, 2020, 21, 72-86.	0.7	6
107	Local electronic transport across probe/ionic conductor interface in scanning probe microscopy. Ultramicroscopy, 2021, 220, 113147.	0.8	6
108	Exploring Charged Defects in Ferroelectrics by the Switching Spectroscopy Piezoresponse Force Microscopy. Small Methods, 2022, 6, 2101289.	4.6	6

#	Article	IF	CITATIONS
109	Exploring the magnetically induced field effect in carbon nanotube-based devices. Physica E: Low-Dimensional Systems and Nanostructures, 2008, 40, 1010-1013.	1.3	5
110	Tunable Microwave Conductance of Nanodomains in Ferroelectric PbZr _{0.2} Ti _{0.8} O ₃ Thin Film. Advanced Electronic Materials, 2022, 8, 2100952.	2.6	5
111	Graphene etching by a Near-Field Scanning Microwave Microscope. , 2013, , .		4
112	Transition layers in metal bilayers produced by pulsed laser deposition in vacuum. Journal of Vacuum Science and Technology A: Vacuum, Surfaces and Films, 2002, 20, 1557-1565.	0.9	3
113	Near field microwave microscopy for nanoscale characterization, imaging and patterning of graphene. , 2014, , .		3
114	Enhancement of local piezoelectric properties of a perforated ferroelectric thin film visualized via piezoresponse force microscopy. Journal Physics D: Applied Physics, 2017, 50, 425303.	1.3	3
115	Probing Electrified Liquid–Solid Interfaces with Scanning Electron Microscopy. ACS Applied Materials & Interfaces, 2020, 12, 56650-56657.	4.0	3
116	Magnetooptical properties of alloy films Co–Pd with perpendicular magnetic anisotropy. Journal of Magnetism and Magnetic Materials, 1999, 203, 244-246.	1.0	2
117	Nonconventional transition layer formation during PLD of nanometer-period multilayers. , 1999, 3687, 244.		2
118	<title>Structural peculiarities of metal alloy and multilayer films synthesized from laser erosion plasma</title> . , 2001, , .		2
119	Patterning: Atomicâ€Level Sculpting of Crystalline Oxides: Toward Bulk Nanofabrication with Single Atomic Plane Precision (Small 44/2015). Small, 2015, 11, 5854-5854.	5.2	2
120	Production of Thin Films of Metastable Materials by Cross-Beam Pulsed Laser Deposition. Materials Science Forum, 2000, 343-346, 231-236.	0.3	1
121	Metastable Phase Formation in Fe-Al Thin Films Cocondensed by Cross-Beam Pulsed Laser Deposition. Materials Science Forum, 2000, 343-346, 249-254.	0.3	1
122	Giant magnetoresistance and magnetism of heterogeneous CoCu produced by ion-beam techniques. Sensors and Actuators A: Physical, 2001, 91, 169-172.	2.0	1
123	Lattice-Symmetry-Driven Phase Competition in Vanadium Dioxide. Materials Research Society Symposia Proceedings, 2011, 1292, 67.	0.1	1
124	Atomic-Level Fabrication of Crystalline Oxides in STEM. Microscopy and Microanalysis, 2015, 21, 939-940.	0.2	1
125	Probing nanoscale objects in liquids through membranes with near-field microwave microscopy. , 2015, , .		1
126	Dielectrophoresis-Based Assembly and High-Frequency Characterization of Carbon Nanotube Bundles. Materials Research Society Symposia Proceedings, 2007, 990, 1.	0.1	0

#	Article	IF	CITATIONS
127	Probing nanotube-based ambipolar FET by magnetic field. AIP Conference Proceedings, 2007, , .	0.3	Ο
128	Unconventional Antiferroelectric Phase Stabilization in Thin Film BiFeO3 by Interface-Induced Rotoelectric Coupling Effect. Microscopy and Microanalysis, 2012, 18, 412-413.	0.2	0
129	Functional material properties of oxide thin films probed by atomic force microscopy on the nanoscale. , 2018, , 181-201.		0
130	Polarization of the Graphene-Liquid Electrolyte Interface Probed by SEM. Microscopy and Microanalysis, 2018, 24, 354-355.	0.2	0
131	Operando Scanning Electron and Microwave Microscopies in Plasmas: A Comparative Analysis. Microscopy and Microanalysis, 2020, 26, 2498-2499.	0.2	0
132	Multiferroic properties of barium strontium titanate ceramics doped with gadolinium and iron. Ferroelectrics, 2021, 574, 109-114.	0.3	0
133	Metastable phase formation and subsequent thermally stimulated relaxation of co-deposited Fe-Cr nanometer films. Acta Crystallographica Section A: Foundations and Advances, 2002, 58, c348-c348.	0.3	0
134	Unveiling the Magnetically Induced Field-Effect in Carbon Nanotubes Devices. Springer Proceedings in Physics, 2008, , 111-113.	0.1	0
135	Electromigration and Diffusion Researches in Scanning Probe Microscopy of Solid Electrolytes. Ukrainian Journal of Physics, 2015, 60, 1027-1035.	0.1	0
136	Correlative Scanning Probe and Confocal Raman Microscopy for the Evaluation of Li-ion Kinetics in LiMn2O4 Cathodes. , 0, , .		0
137	Influence of voltage amplitude parameters on the electrocaloric response in ferroelectric materials. Ferroelectrics, 2022, 591, 43-50.	0.3	Ο